International Conference on Applied Energy 2019
Aug 12-15, 2019, Västerås, Sweden
Paper ID: 582

HIERARCHICAL NANONEEDLE –DECORATED SHELL STRUCTURE OF COBALT PHOSPHIDE AS COUNTER ELECTRODE FOR DYE-SENSITIZED SOLAR CELL

Chia-Lin Yeh [a], Yi-June Huang [a], Han-Ting Chen [a], Chuan-Pei Lee [b], and Kuo-Chuan Ho [a, c, d*]
[a] Department of Chemical Engineering, National Taiwan University, Taipei 10617, Taiwan
[b] Department of Applied Physics and Chemistry, University of Taipei, Taipei 10048, Taiwan
[c] Institute of Polymer Science and Engineering, National Taiwan University, Taipei 10617, Taiwan
[d] Advanced Research Center for Green Materials Science and Technology, National Taiwan University, Taipei 10617, Taiwan

[*] Corresponding Author
E-mail: kcho@ntu.edu.tw; Fax: +886-2-2362-3040; Tel: +886-2-3366-3020

ABSTRACT

The nanoneedle-decorated shell, nanoneedle, and nanosheet structures of cobalt phosphide (named CoP-NDS, CoP-N, and CoP-S, respectively) are synthesized via one-step hydrothermal method and phosphilization process. The CoP-NDS is consisted of nanoneedle with about 400 nm of length and nanosheet with about 100 nm of thickness. The CoP-NDS hierarchical structure provides a larger specific surface area and allows more electrolyte to penetrate into the interior of the nanospace. The result shows that dye-sensitized solar cell (DSSC) using CoP-NDS as the counter electrode (CE) exhibits the best photoelectric conversion efficiency (η) of 8.80 ± 0.07%, as compared to CoP-N (8.50 ± 0.13%) and CoP-S (7.71 ± 0.12%) CEs under the illumination of 1 sun (AM1.5G, 100 mW cm^{-2}). Furthermore, CoP-NDS CE shows higher photovoltaic performance than traditional Platinum (Pt) CE (8.24 ± 0.02%), demonstrating its potential to replace Pt as CE in DSSCs. To further explore the application, the photovoltaic performance of DSSCs under dim light condition is also studied. The results show that DSSCs with CoP-NDS CE achieve η's of 14.22 ± 0.12%, 15.75 ± 0.02%, and 17.27 ± 0.14% at 1000, 3500, and 7000 lux, respectively. This study concludes that the low-cost and easy-to-fabricate CoP-NDS can be a promising candidate to replace the conventional Pt CE in DSSCs.

Keywords: Dim light photovoltaics, dye-sensitized solar cell, nanoneedle, nanosheet, Pt-free counter electrode, transition metal phosphide.

NONMENCLATURE

Abbreviations	
CoP	Cobalt phosphide
CoP-NDS	Nanoneedle-decorated shell structured CoP
CoP-N	Nanoneedle structured CoP
CoP-S	Nanosheet structured CoP
DSSCs	Dye-sensitized solar cells
FTO	Fluorine-doped tin oxide
Pt	Platinum
CE	Counter electrode
V_{OC}	Open-circuit voltage
J_{SC}	Short-circuit current density
FF	Fill factor
DIW	Deionized water
Symbols	
η	efficiency

1. INTRODUCTION

To solve the problem of energy shortage, researches have been focused on energy conversion and storage systems vigorously. Among the current energy conversion systems, photovoltaic system is promising and eco-friendly. Researchers have put efforts to improve the photovoltaic efficiency and reduce the cost of device for commercialization. Due to the low cost, simple fabrication process, less sensitiveness to the angle of incidence, and high efficiency under ambient light illumination, dye-sensitized solar cells (DSSCs) have gained much attentions in photovoltaic field [1], [2]. Typical DSSC is composed of a dye-adsorbing

mesoporous TiO_2 photoanode, electrolyte with iodide/triiodide ions, and a counter electrode (CE). The main function of CE is to receive the electrons from outer circuit and regenerate iodide ions in the electrolyte [3]. Traditionally, Pt is used as the CE in DSSCs because of its high conductivity and electrocatalytic ability. However, due to the scarcity, expensiveness, and corrosion to iodide ion, several high electrocatalytic performance Pt-free materials for CE, such as conducting polymers, carboneous materials, transition metal compounds, and alloys have been developed [4], [5], [6].

Cobalt-based materials possess attractive eletrocatalytic ability and low cost among transition metal compounds. Previous reports show that application of cobalt-based transition metal compounds as CE in DSSCs exhibit high photovoltaic performance [7], [8]. Among these cobalt-based transition metal compounds, CoP has high electrocatalytic ability since the introduction of electronegative P atom results in a lower adsorption free energy for ions in electrolyte [9]. Therefore, CoP has been applied as an electrode material in electrochemical systems, such as hydrogen evolution reactions [10], oxygen evolution reactions [11], supercapacitors [12], and lithium ion batteries [13]. In addition to the superior electrocatalytic ability, CoP can be tailored to obtain various nanostructures via tuning the preparation method and parameter, thereby acquiring high specific surface area and more open space for electrolyte going deep into the interior of the nanospace to make complete usage of the active sites, yielding better electrochemical performance. Several nanostructures of CoP have been reported in literatures, including nanoparticle [14], hollow polyhedron [15], nanoneedle [16], nanosheet [17], and nanoflower [18].

Although CoP has been applied in various electrochemical fields, it has seldom been applied as CE materials in DSSCs. Furthermore, from previous reports applying transition metal compounds as CE, it was found that the difference in nanostructure has significant influence on the photovoltaic performance in DSSCs. Hence, in this study, a hydrothermal method is proposed to synthesize the precursor of CoP. The precursor of CoP was treated with phosphilization process to obtain three different structures of CoP. That is, the influence of one dimensional, two dimensional, and the combination of one and two dimensional structures on the photovoltaic performance in DSSCs would be discussed in this study.

2. EXPERIMENTAL SECTION

2.1 Material

Cobalt sulfate heptahydrate ($CoSO_4 \cdot 7H_2O$), ethanol (EtOH, 99.5%), titanium (IV) tetraisoproproxide (TTIP, >98%), methanol, 2-methoxyethanol were purchased from Sigma Aldrich. Lithium iodide (LiI, synthetical grade), iodine (I_2, synthetical grade) were received from dicarboxylato) ruthenium (II) bis(tetrabutylammonium) (N719 dye), transparent TiO_2 paste (Ti-Nanoxide T/SP, average diameter of 20 nm), and Surlyn® (SX1170-60, 60 μm) were acquired from Solaronix (S.A., Aubonne, Switzerland). 1,2-Dimethyl-3-propylimidazolium iodide (DMPII) was purchased from Tokyo Chemical Industry Co. Ltd. Acetonitrile (ACN, 99.99%), Cobalt nitrate hexahydrate ($Co(NO_3)_2 \cdot 6H_2O$), and urea were purchased from J. T. Baker. Acetone (99%), 4-tert-butylpyridine (tBP, 96%) were purchased from Acros. 3-Methoxypropionitrile (MPN, 99%), hexamethlene tetramine, and Sodium hypophosphite monohydrate ($NaH_2PO_2 \cdot H_2O$) were purchased from Alfa Aesar. The flexible substrate, carbon cloth (W0S1002, thickness = 0.36 mm, basic weight = 120 g cm^{-2}, sheet resistance = 0.60 Ω $sq.^{-1}$) was obtained from CeTech Co., Ltd., Taiwan.

2.2 Synthesis of precursor of CoP-NDS, CoP-N, and CoP-S

For synthesis of precursor of CoP-NDS, the $CoSO_4 \cdot 7H_2O$ and urea were dissolved in methanol and DIW. Subsequently, the uniform solution was transferred to a Teflon vessel for hydrothermal synthesis at 90 °C for 12 h. For comparison, nanoneedle structured and nanosheet structured CoP (CoP-N and CoP-S) were also synthesized. CoP-N was prepared as reported previously [9], the $Co(NO_3)_2 \cdot 6H_2O$ and urea were dissolved in DIW and then the uniform solution was heated at 120 °C for 12 h. CoP-S was also prepared according to literature [16], the $Co(NO_3) \cdot 6H_2O$ and hexamethlene tetramine were dissolved in DIW and the uniform solution was heated at 100 °C for 12 h. All the products were collected by centrifugation under 7000 rpm and washed with DIW for 5 times, dried under vacuum at 60 °C overnight to get the final products.

2.3 Fabrication of the counter electrode

A 50 nm-thick Pt film was deposited on an FTO glass by a direct current sputtering method to prepare Pt CE. The CE with different structures of CoP films were prepared by drop-coating 90 μl of uniform slurry composed of 20 mg powder of precursor and 2 ml DIW onto 1 cm^2 carbon cloth. And then precursor at carbon cloth was heated in a tube furnace with upstream reactant of $NaH_2PO_2 \cdot H_2O$ at 300°C for 1.5 hour with Argon as carrier gas.

2.4 Fabrication of the DSSCs

The TiO_2 photoanode was consisted of compact layer, transparent layer, and scattering layer. For fabrication of compact layer, an uniform solution of tetraisopropoxide (TTIP, > 98%) and 2-methoxyethanol was deposited onto FTO glass by spin-coating method. For fabrication of transparent layer, the commercial transparent TiO_2 paste (Ti-nanoxide HT/SP, average diameter of 20 nm) was coated on the compact layer by the doctor-blade method. For fabrication of scattering layer, we used the same doctor-blade method with home-made TiO_2 slurry. Each layer of photoanode was sintered at 500°C for 30 min in an ambient environment after coating TiO_2. Finally, the prepared photoanode was immersed in a 5 x 10^{-4} M N719 dye solution for 24 hours. The electrolyte was the solution of LiI, I_2, DMPII, and tBP in ACN and MPN. The device of DSSCs were composed of dye-adsorbed TiO_2 photoanode, electrolyte, and a CE. The gap between the photoanode and CE was fixed by a 60 mm-thick Surlyn® ionomer and sealed by heating. Then the electrolyte was injected into the gap to make DSSCs device complete.

2.5 Characterizations and measurement

X-Ray diffraction (XRD) patterns were recorded by Multipurpose X-ray diffraction system (Ultima IV, Rigaku, USA). Surface morphology of various CE were observed by a field-emission scanning electron microscope (FE-SEM, Nova NanoSEM 230, FEI, Oregon, USA). The Brunauer-Emmett-Teller (BET) surface area was measured by a nitrogen sorption isotherm apparatus (Micromeritics, ASAP2010). Photovoltaic parameters of the DSSCs with various CE were measured by a potentiostat/galvanostat (PGSTAT 30, Autolab Eco-Chemie, Utrecht, the Netherlands). The power conversion efficiency of DSSCs were obtained under light illumination of 100 mW cm^{-2}, using a class A quality solar simulator (XES-301S, AM1.5G, San-Ei Electric Co. Ltd., Osaka, Japan). The incident light intensity was calibrated with a standard Si cell (PECSI01, Peccell Technologies, Inc., Kanagawa, Japan).

3. RESULTS AND DISCUSSION

3.1 Structural Analysis

The crystalline phases of CoP-NDS, CoP-N, and CoP-S are confirmed by the X-ray diffraction (XRD) patterns as shown in Fig. 1 The XRD patterns show that all structures of CoP exhibit 31.6° (011), 36.3° (111), 46.2° (112), 48.1° (211), and 56.8° (301) diffraction peaks of the orthorhombic CoP phase (JCPDS No. 29-0497) [14]. The results show that all structures of CoP are successfully obtained from precursor via phosphilization process.

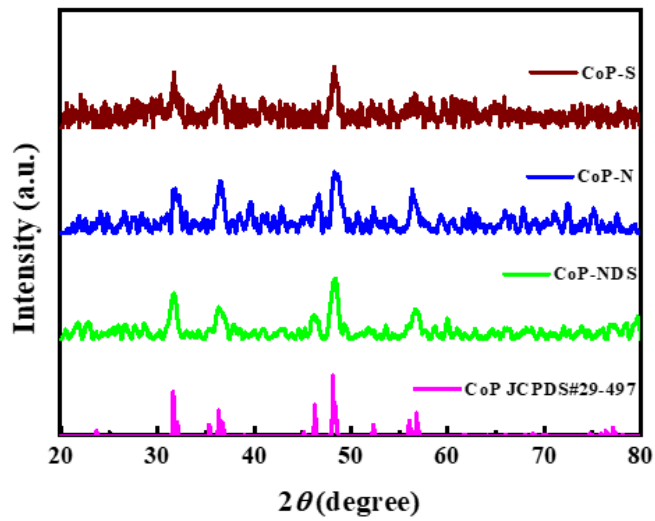

Fig. 1. XRD patterns of CoP-NDS, CoP-N, and CoP-S.

3.2 Morphologies Analysis

Fig. 2 shows the FE-SEM images of CoP-NDS, CoP-N, and CoP-S, which are systematically synthesized to study the effect of structure on the photovoltaic performance of DSSCs. According to Fig. 2(a), the CoP-NDS is composed of nanoneedle decorated nanosheet and the nanosheet further assembles to be a sphere-like structure. Among them, the nanoneedle has about 400 nm of length and nanosheet has about 100 nm of thickness. In Fig. 2(b), the CoP-N possesses about 12 µm of length and about 20 nm of diameter. The CoP-S reveals about 100 nm of thickness and about 8 µm of width (Fig. 2(c)). The FE-SEM images suggest that the CoP-NDS has a high specific surface area with large open space, presumably due to its vertically hierarchical structure. Furthermore, the precise specific surface area of the CoP-NDS, CoP-N, and CoP-S are confirmed by the Brunauer-Emmett-Teller (BET) analysis. The BET specific urface areas of CoP-NDS, CoP-N, and CoP-S are 148.83 ± 1.26 m^2/g, 60.14 ± 0.23 m^2/g, and 44.37 ± 0.24 m^2/g, respectively. These data verify that the nanoneedle-decorated shell structure can provide a higher specific surface area than that of nanoneedle or nanosheet structure.

3.3 Photovoltaic performance

Fig. 3 shows the J-V curves of the DSSCs fabricated with Pt, CoP-NDS, CoP-N, and CoP-S CEs under 1 sun

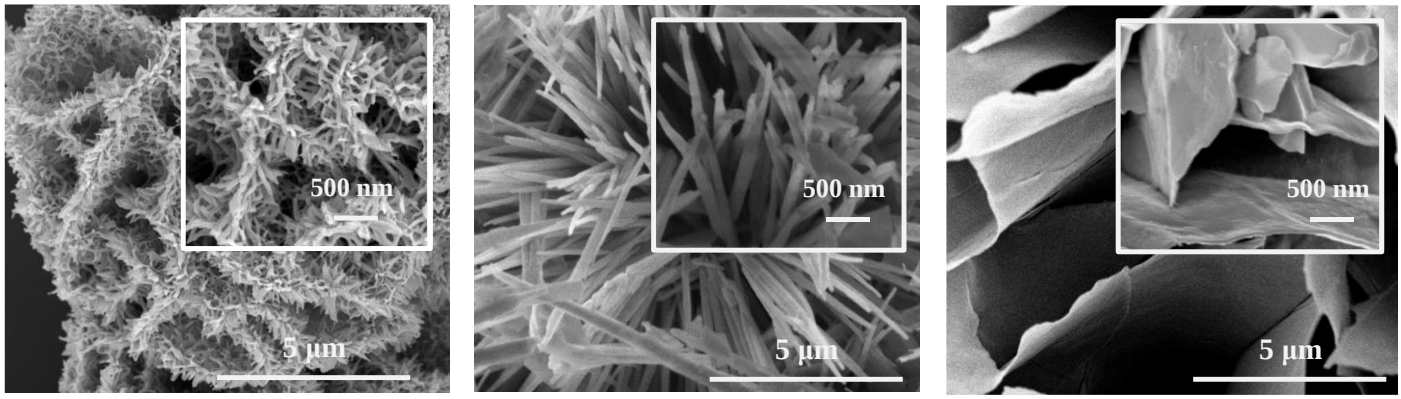

Fig. 2. FE-SEM images of (a) CoP-NDS (b) CoP-N, and (c) CoP-S.

illumination. The corresponding photovoltaic parameters are listed in Table 1.

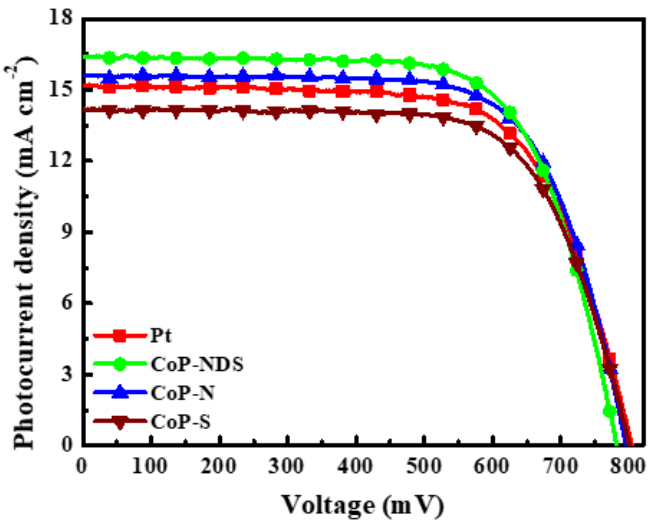

Fig. 3. Photocurrent density-voltage curve of DSSCs with various CEs under 1 sun illumination.

The DSSCs with CoP-NDS CEs show an average efficiency (η) of 8.80 ± 0.07% with an open-circuit voltage (V_{OC}) of 773.77 ± 5.27 mV, a short-circuit current density (J_{SC}) of 16.50 ± 0.10 mA cm^{-2}, and a fill factor (FF) of 0.70 ± 0.01. Its η is the highest as compared to CoP-N (8.50 ± 0.13%) and CoP-S (7.71 ± 0.12%) CEs. Moreover, the performance of CoP-NDS CE is better than the Pt CE (8.24 ± 0.02%). It can be found that high active area and conductivity of CoP-NDS would allow DSSC to have higher values of J_{SC} and FF. For comparison of different structures of CoP CEs, the values of J_{SC} for CoP-NDS, CoP-N, and CoP-S are 16.50 ± 0.10 mA cm^{-2}, 15.34 ± 0.19 mA cm^{-2}, and 13.95 ± 0.17 mA cm^{-2}, respectively. The CoP-NDS has the highest J_{SC} among different structures of CoP. The order of J_{SC} (CoP-NDS > CoP-N > CoP-S) can be attributed to the specific surface area and morphology characteristic of different structures. As the BET specific surface area mentioned above, the order of BET specific surface area can be straightforwardly regarded as the relative amount of active sites of different structure of CoP to reduce the triiodide ion of electrolyte and finally results in the order of J_{SC}. And then from Fig. 2(a), we can find the CoP-NDS is composed of both nanoneedle and nanosheet structure. That is to say that the CoP-NDS combines both advantages from each structure and make it acquire the highest J_{SC}.

To further investigate the efficiency of the best DSSC under dim-light condition, the J-V curves of the DSSCs with CoP-NDS CEs are shown in Fig. 4 at a light irradiance of 2.20 mW cm^{-2} (7000 lux), 1.08 mW cm^{-2} (3500 lux), and 0.33 mW cm^{-2} (1000 lux). And the corresponding results are listed in Table 2. The DSSC using the CoP-NDS CE exhibits an average ηs of 14.22 ± 0.12%, 15.75 ± 0.02%, and 17.27 ± 0.14% under 1000 lux, 3500 lux, and 7000 lux illumination, respectively. The results show that DSSCs with CoP-NDS CE can operate well and obtain high efficiency under indoor condition.

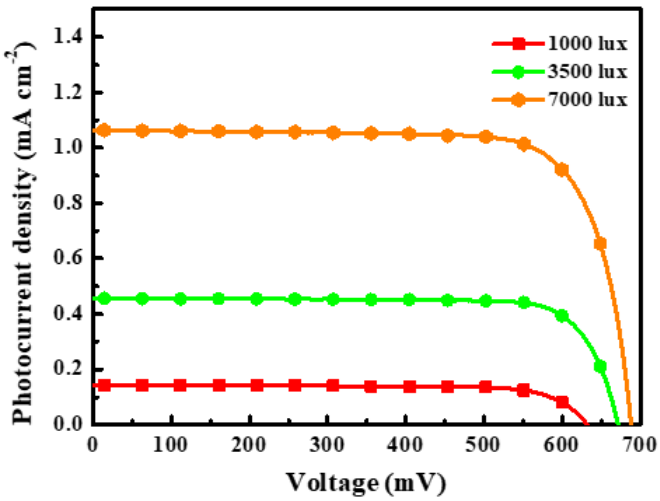

Fig. 4. Photocurrent density-voltage curve of DSSCs with the CoP-NDS CE under dim light condition.

Table 1. Photovoltaic parameters of the DSSCs with various CEs, measured at 100 mW cm^{-2} (AM 1.5G, 1 sun). The standard deviation for each data is based on three DSSCs.

	V_{OC} (mV)	J_{SC} (mA cm^{-2})	FF	η (%)
CoP-NDS	773.77 ± 5.27	16.50 ± 0.10	0.70 ± 0.01	8.80 ± 0.07
CoP-N	785.98 ± 5.27	15.34 ± 0.19	0.70 ± 0.00	8.50 ± 0.13
CoP-S	790.86 ± 5.27	13.95 ± 0.17	0.70 ± 0.01	7.71 ± 0.12
Pt	800.63 ± 1.99	15.19 ± 0.02	0.67 ± 0.00	8.24 ± 0.02

3.4 Long-term stability

To further investigate the stability of the CoP-NDS and Pt CE, cyclic voltammetry data up to 500 cycles from -0.9 to 0.6 V (vs. Ag/Ag^+) at a scan rate of 100 mV/s were obtained. Fig. 5 shows the normalized cathodic peak current density (J_{PC}) at various cycle numbers for CoP-NDS and sputtered Pt CE. After 500 cycles of cyclic voltammetry, the CoP-NDS CE maintains 68% of its initial peak current density, while the sputtered Pt CE retains only 45% of its initial value. It is generally accepted that Pt would be corroded by triiodide ion and the formation of PtI_4 would dramatically decrease the electrocatalytic ability [18], thus leading to the poorer long-term stability than that of the CoP-NDS CE.

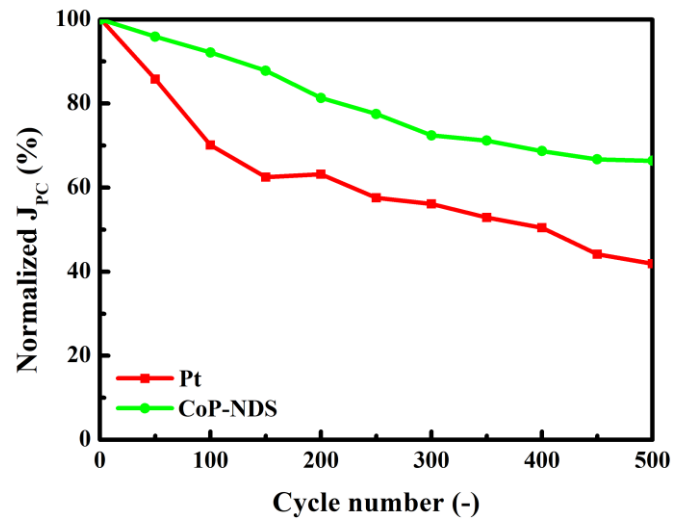

Fig. 5. Long-term stability data for the CoP-NDS and Pt CE obtained from cyclic voltammetry.

4. CONCLUSION

Nanoneedle-decorated shell, nanoneedle and nanosheet structures of CoP are successfully synthesized via one-step hydrothermal method and phophilization process. These were further applied as Pt-free CEs in DSSCs. The FE-SEM images reveal that nanoneedle-decorated shell, nanoneedle and nanosheet structures of CoP are successfully synthesized and their crystalline phases are confirmed by XRD analysis. The CoP-NDS offers the highest cell efficiency of 8.80 ± 0.07% as compared to CoP-N and CoP-S and further exceeds the efficiency of a Pt CE. Furthermore, DSSC with CoP-NDS CE also shows a high η under dim light condition. From the results mentioned above, the high efficiency and low cost render CoP-NDS a promising candidate to replace traditional Pt CE in DSSCs.

ACKNOWLEDGEMENT

This work was financially supported by the "Advanced Research Center for Green Materials Science and Technology" from The Featured Area Research Center Program within the framework of the Higher

Table 2. Photovoltaic parameter of the DSSCs with CoP-NDS CE, measured at 1000 lux, 3500 lux, and 7000 lux. The standard deviation for each data is based on three DSSCs.

Illuminance (lux)	V_{OC} (mV)	J_{SC} (mA cm^{-2})	FF	η (%)	P_{in} (mW cm^{-2})
1000	631.71 ± 0.00	0.09 ± 0.00	0.77 ± 0.00	14.22 ± 0.12	0.33
3500	672.40 ± 1.15	0.31 ± 0.00	0.80 ± 0.00	15.75 ± 0.02	1.08
7000	687.05 ± 1.15	0.72 ± 0.01	0.77 ± 0.00	17.27 ± 0.14	2.20

Education Sprout Project by the Ministry of Education (107 L9006) and the Ministry of Science and Technology in Taiwan (MOST 107-3017-F-002-001). This work was also partially sponsored by the Academia Sinica, Nankang, Taipei, Taiwan (2019 Sustainability Science Research Project, AS-SS-108-02) and the Ministry of Science and Technology (MOST) of Taiwan, under grant numbers 103-2119-M-007-012, and 105-2221-E-002-229-MY3.

REFERENCE

[1] Lee C-P, Lin C-A, Wei T-C, Tsai M-L, Meng Y, Li C-T, et al. Economical low-light photovoltaics by using the Pt-free dye-sensitized solar cell with graphene dot/PEDOT:PSS counter electrodes. Nano Energy 2015;18:109-17.

[2] Freitag M, Teuscher J, Saygili Y, Zhang X, Giordano F, Liska P, et al. Dye-sensitized solar cells for efficient power generation under ambient lighting. Nat. Photonics. 2017;11:372-8.

[3] Wu J, Lan Z, Lin J, Huang M, Huang Y, Fan L, et al. Counter electrodes in dye-sensitized solar cells. Chem. Soc. Rev. 2017;46:5975-6023.

[4] Ahmed U, Alizadeh M, Rahim NA, Shahabuddin S, Ahmed MS, Pandey AK. A comprehensive review on counter electrodes for dye sensitized solar cells: A special focus on Pt-TCO free counter electrodes. Sol. Energy 2018;174:1097-125.

[5] Gao C, Han Q, Wu M. Review on transition metal compounds based counter electrode for dye-sensitized solar cells. J. Energy Chem. 2018;27:703-12.

[6] Chen M, Shao L-L. Review on the recent progress of carbon counter electrodes for dye-sensitized solar cells. Chem. Eng. J. 2016;304:629-45.

[7] Huang Y-J, Lee C-P, Pang H-W, Li C-T, Fan M-S, Vittal R, et al. Microemulsion-controlled synthesis of CoSe2/CoSeO3 composite crystals for electrocatalysis in dye-sensitized solar cells. Materials Today Energy 2017;6:189-97.

[8] Kang J-S, Kim J-Y, Yoon J, Kim J, Yang J, Chung D-Y, et al. Room-Temperature Vapor Deposition of Cobalt Nitride Nanofilms for Mesoscopic and Perovskite Solar Cells. Adv. Energy Mater. 2018;8:1703114.

[9] Liu T, Xie L, Yang J, Kong R, Du G, Asiri AM, et al. Self-Standing CoP Nanosheets Array: A Three-Dimensional Bifunctional Catalyst Electrode for Overall Water Splitting in both Neutral and Alkaline Media. ChemElectroChem 2017;4:1840-5.

[10] Popczun EJ, Read CG, Roske CW, Lewis NS, Schaak RE. Highly Active Electrocatalysis of the Hydrogen Evolution Reaction by Cobalt Phosphide Nanoparticles. Angew. Chem., Int. Ed. 2014;53:5427-30.

[11] Zhang G, Wang B, Bi J, Fang D, Yang S. Constructing ultrathin CoP nanomeshes by Er-doping for highly efficient bifunctional electrocatalysts for overall water splitting. J. Mater. Chem. A 2019;7:5769-78.

[12] Elshahawy AM, Guan C, Li X, Zhang H, Hu Y, Wu H, et al. Sulfur-doped cobalt phosphide nanotube arrays for highly stable hybrid supercapacitor. Nano Energy 2017;39:162-71.

[13] Jiang J, Zhu K, Fang Y, Wang H, Ye K, Yan J, et al. Coralloidal carbon-encapsulated CoP nanoparticles generated on biomass carbon as a high-rate and stable electrode material for lithium-ion batteries. J. Colloid Interface Sci. 2018;530:579-85.

[14] Liu M, Li J. Cobalt Phosphide Hollow Polyhedron as Efficient Bifunctional Electrocatalysts for the Evolution Reaction of Hydrogen and Oxygen. ACS Appl. Mater. Interfaces. 2016;8:2158-65.

[15] Xu K, Cheng H, Lv H, Wang J, Liu L, Liu S, et al. Controllable Surface Reorganization Engineering on Cobalt Phosphide Nanowire Arrays for Efficient Alkaline Hydrogen Evolution Reaction. Adv. Mater. 2018;30:1703322.

[16] Chang J, Liang L, Li C, Wang M, Ge J, Liu C, et al. Ultrathin cobalt phosphide nanosheets as efficient bifunctional catalysts for a water electrolysis cell and the origin for cell performance degradation. Green Chem. 2016;18:2287-95.

[17] Fan X, Wang X, Yuan W, Li C-M. Diethylenetriamine-mediated self-assembly of three-dimensional hierarchical nanoporous CoP nanoflowers/pristine graphene interconnected networks as efficient electrocatalysts toward hydrogen evolution. Sustainable Energy Fuels 2017;1:2172-80.

[18] Espen O, Georg H, Sten E-L. Dissolution of platinum in methoxy propionitrile containing LiI/I_2. Sol. Energy Mater. Sol. Cells. 2000;63:267-73